Focusing Forward Genetics: A Tripartite ENU Screen for Neurodevelopmental Mutations in the Mouse

R. W. Stottmann,* J. L. Moran,*,[1] A. Turbe-Doan,* E. Driver,[†] M. Kelley,[†] and D. R. Beier*,[2]

*Division of Genetics, Department of Medicine, Brigham and Women's Hospital, Harvard Medical School, Boston, Massachusetts 02115 and [†]Developmental Neuroscience Section, National Institute for Deafness and Other Communicative Disorders, Bethesda, Maryland 20892

ABSTRACT The control of growth, patterning, and differentiation of the mammalian forebrain has a large genetic component, and many human disease loci associated with cortical malformations have been identified. To further understand the genes involved in controlling neural development, we have performed a forward genetic screen in the mouse (*Mus musculus*) using ENU mutagenesis. We report the results from our ENU screen in which we biased our ascertainment toward mutations affecting neurodevelopment. Our screen had three components: a careful morphological and histological examination of forebrain structure, the inclusion of a retinoic acid response element-lacZ reporter transgene to highlight patterning of the brain, and the use of a genetically sensitizing locus, *Lis1/Pafah1b1*, to predispose animals to neurodevelopmental defects. We recovered and mapped eight monogenic mutations, seven of which affect neurodevelopment. We have evidence for a causal gene in four of the eight mutations. We describe in detail two of these: a mutation in the planar cell polarity gene *scribbled homolog* (*Drosophila*) (*Scrib*) and a mutation in *caspase-3* (*Casp3*). We find that refining ENU mutagenesis in these ways is an efficient experimental approach and that investigation of the developing mammalian nervous system using forward genetic experiments is highly productive.

THE early stages of mammalian forebrain development involve early tissue patterning events followed by an exquisitely coordinated series of cell division and differentiation events. The mammalian telencephalon develops from the most rostral portion of the developing neural tube at very early embryonic stages and ultimately gives rise to the neocortex, hippocampus, olfactory bulbs, and basal ganglia. A precise regional regulation of proliferation (and cell death) is crucial for ultimately creating the proper brain architecture. After terminal division and acquisition of neuronal identity, neural cells must migrate via long, and often circuitous, routes to their final destination and begin the processes of synapse and circuit formation. All of the above events require a wide variety of cell biological processes to occur with high fidelity. While a clearer understanding of the genetic regulation of forebrain development is slowly emerging, much remains to be discovered. Further understanding the formation of the brain will likely help to decipher the causes of many brain diseases (Herron *et al.* 2002), including developmental disorders, degenerative diseases of adult life, and tumorigenesis.

One particularly powerful approach to understanding human gene function is the study of the mouse. Murine anatomy and physiology are very similar to that of humans, and there are significant genetic tools available in the mouse. While genetics in the mouse has generally been extremely informative for developmental biology, it is perhaps surprising that relatively few mouse mutants are informative for the many complex processes of brain patterning. This may be because many of the genes required for brain patterning have roles in early embryonic development, leading to death or significant phenotypes that preclude later analysis of forebrain patterning [*e.g.*, *Fgf8* (Meyers *et al.* 1998), *Shh* (Chiang *et al.* 1996), and *Bmpr1a* (Mishina *et al.* 1995)]. Consequently, crucial neurodevelopmental genes are not easily studied at organogenic stages.

In an attempt to learn more about the molecular regulation of mammalian neurodevelopment, we have performed a screen of mice treated with ENU for recessive, monogenic mutations. The treatment of mice with ENU is an highly effective means for generating heritable changes in the genome with low morbidity and/or mortality (Stottmann

doi: 10.1534/genetics.111.126862
Manuscript received January 14, 2011; accepted for publication April 13, 2011
[1]Present address: Stanley Center for Psychiatric Genetics, Broad Institute of MIT and Harvard, Cambridge, MA 02142.
[2]Corresponding author: Brigham and Women's Hospital/Harvard Medical School, 77 Ave. Louis Pasteur, Boston, MA 02115. E-mail: beier@receptor.med.harvard.edu

and Beier 2010). Lines of mutagenized mice can be efficiently screened for mutations causing organogenic phenotypes (Herron *et al.* 2002). Previous experiments have shown that mutagenesis can uncover mutations affecting the late embryonic brain (Herron *et al.* 2002; Zarbalis *et al.* 2004), but the tissue is complex and not easily examined using histology or molecular analysis. We sought to determine if ENU mutagenesis can be used in a more tissue-specific manner and have taken three complementary approaches to enrich our screen for mutations specifically affecting forebrain development. We have performed morphological and histological analysis of the forebrain, incorporated a reporter allele to highlight the development of distinct structures in the developing forebrain, and genetically sensitized the mutagenized population to increase the incidence of neurodevelopmental defects.

Here we report the results of this mutagenesis experiment where we mapped eight monogenic mutations, seven of which have significant neurodevelopmental defects. All of these are mapped, and we report the causal locus for four. We further describe two of our mutations. One is a new allele of *scribbled homolog* (*Drosophila*) (*Scrib*), which carries a mutation in a potentially informative region of the protein. We also report a new allele of *caspase-3* (*Casp3*), a regulator of apoptosis crucial for neural and craniofacial development. Finally, we also discuss the success of each attempt to bias the screen toward neurodevelopmental phenotypes.

Materials and Methods

Mutagenesis and breeding

ENU mutagenesis followed standard protocols (Stottmann and Beier 2010). In brief, 6- to 8-week-old A/J mice (Jackson Labs) were injected i.p. with a fractionated dose of ENU once weekly for 3 weeks with 90, 95, or 100 mg/kg ENU (Sigma). A/J mice were used due to their ability to tolerate larger doses of ENU with acceptable morbidity and mortality, thus increasing their mutation load and increasing productivity of the screen (Weber *et al.* 2000). ENU was prepared using standard methods and dissolved in ethanol. After allowing for a period of infertility following the mutagenesis, a standard three-generation breeding scheme was followed (Bode *et al.* 1988; Herron *et al.* 2002; also see Results and Figure 1). The A/J males were crossed with FVB/J females (Jackson Labs), retinoic acid response element (RARE)-lacZ–positive females, or *Lis1* heterozygous females (largely from a 129 background). The resulting G2 females were backcrossed to generate G3 embryos or postnatal day (P) 14 pups. For timed pregnancies, successful matings were identified by the presence of a copulation plug, and noon of the day of detection was set as embryonic day (E) 0.5. All animals were housed in accordance with the Harvard Medical School Center for Animal Resources and Comparative Medicine.

Mouse genotyping

RARE-lacZ mice were genotyped with standard lacZ primers (F-TTTAACGCCGTGCGCTGTTCG, R-GATCCAGCGATACAGC GCGTC). *Lis1* heterozygotes were identified using primers for the neomycin resistance cassette (F-TCCTGCCGAGAAAGTATC CATCAT, R-CCAGCCGGCCACAGTCGT) as previously described (Hirotsune *et al.* 1998). Looptail mice carry a mutation in the *vang-like 2* (*Vangl2*) gene, and heterozygous mice were identified by their abnormally looped tail. Direct sequencing of the mutation (in the eighth exon of *vangl2*) was done to genotype embryos (F-AGAGGATGAAGGGTGGGTG, R-GTGTCAGGGCCAGAGAACC).

Whole-genome single nucleotide polymorphism scanning

To map our mutations, we genotyped a custom whole-genome panel of 768 single nucleotide polymorphism (SNPs) with the Illumina GoldenGate technology at the Broad Institute Center for Genotyping and Analysis. A total of 256 of the 768 SNPs on this panel were polymorphic between A/J and FVB/J. The initial genomic interval carrying the mutation was defined by flanking SNPs, which identified a homozygous A/J haplotype shared by all affected animals. Fine mapping was done by analyzing further meioses with microsatellite markers, restriction fragment length polymorphisms [identified via the MGI database http://www.informatics.jax.org/strains_SNPs.shtml or the algorithm SNP2RFLP (Beckstead *et al.* 2008)], or direct sequencing of SNPs. Sequencing of candidate genes was done with standard methods, either exon-based sequencing or using random-primed cDNA from mutant RNA for transcript analysis. Primer design was either with Primer3 (http://frodo.wi.mit.edu/primer3/) or via the Exon Primer function in the University of California at San Francisco (UCSC) Genome browser (http://genome.ucsc.edu/). All DNA sequencing other than SNP mapping was done at the Dana-Farber/Harvard Cancer Center DNA Resource Core. In two of these mutant lines, *crn2* and *hith2*, our initial mapping was with a cohort of affected animals with multiple phenotypes and resulted in two candidate regions. Analysis of more embryos and standard microsatellite mapping demonstrated that not all phenotypes were allelic and allowed us to focus on the chromosomal location reported in Table 2 for mapping *crn2* and *hith2*.

Histology and immunohistochemistry

Histological analysis used standard methods (Nagy 2003). Embryos were fixed in either Bouin's fixative or 4% paraformaldehyde followed by paraffin embedding and sectioning at 14 μm. Sections were stained with hematoxylin and eosin or Cresyl violet. Caspase-3 immunohistochemistry was performed on paraffin sections following the manufacturer's instructions using reagents described below. After deparaffinization of the slides, antigen retrieval was performed with Citra Buffer (Biogenex). Blocking against background from avidin–biotin immunohistochemistry was done with

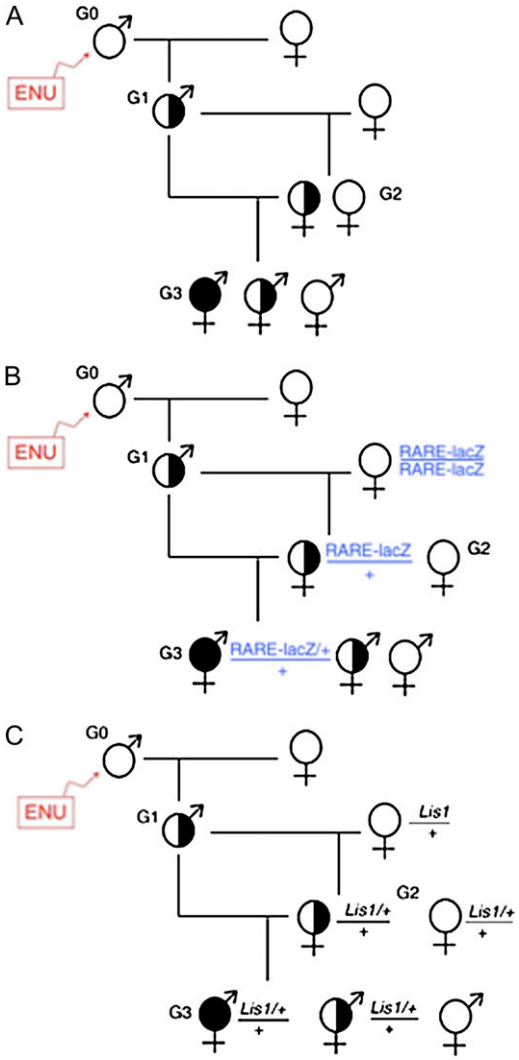

Figure 1 ENU breeding scheme. (A) A traditional three-generation breeding scheme for recovering recessive traits in the third generation (G3). G0 males are mutagenized and outcrossed to generate the G1 population. These are again outcrossed to generate G2 females, which may carry any given ENU mutation. These are backcrossed to the G1 male to create the G3 generation, which is then screened for phenotype(s). Solid indicates homozygosity for an ENU mutation, open indicates no mutation, solid/open indicates heterozygosity. (B) Introduction of a reporter allele is accomplished by mating RARE-lacZ–positive animals to the G1 male and genotyping subsequent females for the transgene. (C) Similarly, a sensitizing locus is incorporated by mating *Lis1* heterozygous females with G1 males.

commercial reagents (DAKO, Vectorlab). Slides were incubated with a primary antibody against full-length caspase-3 (Cell Signaling) overnight at 4° at 1:200. Visualization was with a biotin-labeled secondary antibody (Vectastain Universal ABC kit) and counterstained with hematoxylin QS (Biogenex).

Analysis of crn2 cochlear phenotype

E18 whole-mount cochleae were fixed in 4% paraformaldehyde, dissected to expose the sensory epithelium, and stained with Alexa Fluor-conjugated phalloidin (1:200; Invitrogen). Images shown are confocal projections of the cochlear sensory epithelium. Absolute rotation of hair-cell stereocilia bundles was assessed at positions of 5, 25, and 50% of the total cochlear length from the basal end of the duct, as previously described (Montcouquiol *et al.* 2003). Data are presented as the average deviation from 0°; error bars represent SEM. Significant differences were determined by two-tailed *t*-test.

Results

Screen design

We performed an independent ENU mutagenesis experiment in a similar manner to our previous experiments done with the goal of obtaining novel mouse mutations that model human congenital defects (Herron *et al.* 2002). We used a standard three-generation breeding scheme designed for the recovery of recessive traits (McDonald and Bode 1988; Kasarskis *et al.* 1998; Herron *et al.* 2002; Figure 1). An initial population of mice (G0) was treated with ENU to induce random single nucleotide mutations throughout the animals, including the germline. These were used to create male offspring (G1), each of which will carry some proportion of the mutations in the paternal gametes. The G1 male animals are again outcrossed to create the G2 generation, each member of which has a 50% chance of carrying any specific mutation. The G2 female progeny are then mated back to the G1 males in an attempt to homozygose an ENU mutation in the G3 generation. These embryos are analyzed for gross morphological abnormalities at E18.5, one day before birth, which allows for significant organogenesis and the development of phenotypes that would be lethal upon birth (Herron *et al.* 2002). We have found this strategy to be useful for the discovery of phenotypes that model defects found in human populations (Ackerman *et al.* 2005). As in our previous studies (Herron *et al.* 2002), we have performed the mutagenesis breeding as an outcross. We mutagenized males from an A/J background and crossed to FVB/J females to create the G1 generation. The G2 generation was again generated with an FVB/J outcross. This strategy ultimately creates genetically heterogeneous G3 embryos, which are informative for mapping purposes.

We used three distinct strategies to perform our phenotypic analysis in efforts to more specifically query neurodevelopment. First, embryos were carefully examined for gross phenotypes with an initial examination to assess overall body patterning, including features such as head size and appearance, limb patterning, digit number, and tail morphology (Figure 1A). This was followed by removal of the brain from the skull for a more detailed examination, noting such features as presence/absence of the anterior-most olfactory bulbs, size and location of the telencephalic vesicles, and midbrain/hindbrain structures. Each brain was then embedded in paraffin and sectioned in the coronal plane to more carefully examine the cortical architecture.

Table 1 Results of ENU mutagenesis screening

Type of screening	Lines established	No. of lines completely analyzed	Litters	Mice	Mapped mutations	Grossly visible mutations	Forebrain affected
Morphological	52	17	245	2322	4	3	3
RARE-lacZ	16	14	176	1344	2[a]	2	2
Lis1 sensitized, P14	8	7	114	545	2[b]	2	2
Total	76	38	535	4211	8	7	7

[a] Neither of these phenotypes were discovered with the LacZ reporter transgene.
[b] Neither of these phenotypes were dependent on *Lis1* heterozygosity.

While this style of gross embryonic phenotyping has been fruitful (Kasarskis *et al.* 1998; Herron *et al.* 2002) and has yielded interesting neurodevelopmental mutations, it is difficult to observe any fine detail in brain development using this approach. Histological or immunohistochemical analysis is potentially useful but may reduce the efficiency of screening. Another technique commonly used in mutagenesis experiments in flies and worms has been to incorporate a transgenic "reporter" allele, which highlights a structure of interest that would not otherwise be visible to the investigator. Thus, the sensitivity of the screen is greatly enhanced by employing either a simple histochemical reaction or visualization using fluorescence microscopy. We chose to use the RARE-lacZ transgenic mouse line (Rossant *et al.* 1991) to highlight several structures in the brain that we would otherwise not be able to readily score, including the optic nerves and hippocampus (Figure 1B). The RARE-lacZ transgene contains a retinoic acid response element immediately upstream of a β-galactosidase reporter cassette and is expressed in a gradient from low levels rostrally to high levels caudally in the forebrain (Luo *et al.* 2004). We chose the RARE-lacZ reporter allele for these expression patterns in discrete regions of the brain, not as part of a screen designed to obtain alleles with a role in retinoic acid signaling. The use of a lacZ-based reporter instead of GFP offers some flexibility in phenotyping the embryos, which can be useful when large numbers of embryos are dissected at once.

In a further attempt to enrich our screen for defects in neurodevelopment, we employed an approach commonly used in invertebrate mutagenesis experiments, but less commonly used in mammalian studies: the incorporation of a mouse carrying a mutation that genetically sensitizes, or predisposes, our mutagenized population toward defects in cortical development (Figure 1C). Mutations in *Lis1* (*Pafah1b1*) cause lissencephaly (smooth brain) and neural migration defects in both mice and humans (Reiner *et al.* 1993; Hirotsune *et al.* 1998; Gambello *et al.* 2003). Previous work has shown that *Lis1* interacts genetically with several components of reelin signaling (Assadi *et al.* 2003), an essential pathway for cortical development. Mice heterozygous for mutations in *Lis1* have a low incidence of hydrocephalus (7%) (Assadi *et al.* 2003). The incidence of hydrocephaly is dramatically increased when heterozygosity for *Lis1* is combined with mutations in any one of several genes in the reelin pathway [*e.g.*, 85% in *rl/rl;lis1/+* animals (Assadi *et al.* 2003)]. We hypothesized that, by analyzing ENU mutations on a background with reduced *Lis1* gene function, we may identify more components of the reelin pathway as well as other genes essential for normal brain development. That is, the heterozygous *Lis1* mice represent a *sensitized* background, which will facilitate the identification of other loci that affect neuronal migration. The hydrocephalus phenotype is easily ascertained, making this approach logistically simple and amenable for the analysis of large numbers of progeny. We therefore allowed G3 animals from this arm of the screen to be born and we scored for hydrocephalic pups at P14. This approach was particularly attractive, given that interactions with a heterozygous *Lis1* allele were observed for both heterozygous and homozygous mutations at the secondary locus, which could markedly enhance the yield of the screen (Assadi *et al.* 2003).

All three of these approaches (gross examination, inclusion of a reporter, or sensitizing allele) can be used with the same cohort of G1 animals. There is no difference between the breeding strategies until the mating of G1 males to create the G2 females (Figure 1). Furthermore, if mice carrying a modifying allele (reporter or sensitizing) locus can be bred to homozygosity, this precludes the need to genotype the G2 offspring females for that allele.

Screen results

In this study, 76 G1 males were bred, 52 independent lines (pedigrees) were established, 4211 G3 progeny were screened from 535 litters, and 38 lines were comprehensively analyzed (Table 1). We consider an examination of three or more litters of at least eight embryos a comprehensive analysis, as this provides an ~80% likelihood of identifying a fully penetrant monogenic mutation (Stottmann and Beier 2010). Fourteen abnormal phenotypes were found, of which 8 behaved as heritable monogenic traits (Table 2). These have all been mapped, and the mutant gene is identified for 4. Seven of these phenotypes affected development of the embryonic nervous system, and several of these are likely to be either novel genes or mutations in genes not previously known to be required for neurodevelopment.

Most mutant mice were identified by morphological or histological analysis. In the second arm of the screen in which we employed a *lacz* reporter, 1344 mice from 176 litters (16 lines) were screened, and 12 mice from multiple lines with abnormal lacZ expression profiles were identified. However, the RARE-lacZ reporter allele that we used in this screen was found to have significant variability in

Table 2 ENU mutations recovered

Name	Phenotype description	Chromosome	Interval (Mb)	Locus
Brain dimple (*brdp*)	Telencephalic dysmorphology; mild hydrocephaly	13	15–47 (3)	—
Cleft lip and palate, exencephaly (*clpex*)	Cleft lip and palate, exencephaly	7	81–125 (4)	—
Cleft palate 1 (*clft1*)	Cleft palate only	1	183–197 (10)	*Irf6*
Rudolph (*rud*)	Cortical dysmorphology, shortened long bones	1	160–180 (8)	*Hsd17b7*
Craniorachischisis (*crn2*)	Craniorachischisis	15	49–100 (4[a])	*Scrib*
Progressive hydrocephalus (*prh*)	Progressive hydrocephaly	3	0–76 (4)	—
Cleft face (*clft3*)	Midline fusion defect, small brain, encephalocele	15	0–73 (4)	—
Hole in the head 2 (*hith2*)	Encephalocele, hydrocephalus	8	36–74 (4[a])	*Casp3*

Eight monogenic mutations were recovered in this screen. The causal gene or initial mapping interval from the whole-genome SNP scan is reported with the number of mutants used in parentheses.
[a] See Materials and Methods for details on *Scrib* and *Casp3* mapping.

expression as we introduced different genetic backgrounds during the course of the breeding scheme in Figure 1B, and none of the abnormal phenotypes identified by the reporter proved consistent and heritable. This effect of genetic background on gene expression has been noted before in the mouse genetics literature (*e.g.*, Hebert and Mcconnell 2000).

In the third arm of the screen, we analyzed 545 mice from 114 litters (eight lines). Using this approach, we identified two lines with obvious postnatal defects, including the hydrocephalus phenotype that we hoped to ascertain. However, neither of these phenotypes proved to be dependent on simultaneous heterozygosity for the *Lis1* allele; that is, neither occurred as a consequence of a genetic interaction with the sensitizing allele.

Crn2 is a novel allele of *Scrib*

A mutation identified via gross embryonic examination was the *craniorachischisis 2* (*crn2*) mutation. Most *crn2* embryos ($n = 32$) had an open neural tube along the entire extent of the anterior–posterior axis and a kinked tail (Figure 2, B and D). We also noted exencephaly in a few embryos (both *crn2/+* heterozygotes and homozygotes). Our initial genetic interval included *Scrib*, a known planar cell polarity (PCP) gene, which we considered as a candidate locus on the basis of the similarity of the *crn2* phenotype to published alleles (Rachel *et al.* 2000; Murdoch *et al.* 2001; Zarbalis *et al.* 2004). Sequencing of the *crn2* transcripts revealed a missense mutation in the 19th exon of the *Scrib* transcript, converting a highly conserved glutamic acid residue at position aa 800 to glycine (Figure 2, E–G). The minimal interval from our initial mapping data also included the gene *cadherin*, *EGF LAG seven-pass G-type receptor 1* (*flamingo homolog*) (*Drosophila*) (*Celsr1*). *Celsr1* mouse mutants also have PCP defects, including craniorachischisis. However, sequence analysis of recombinant mice with the *crn2* phenotype identified heterozygous SNPs in *Celsr*, which excluded it from the minimal interval, supporting our conclusion that this mutation in *Scrib* is almost certainly the causal gene in the *crn2* mutant.

We performed two experiments to determine the extent of PCP perturbation and expressivity of this allele. First, we performed a cross with the *looptail* (*Lp*) allele of *vang-like 2* (*Vangl2*), another known PCP gene. A strong interaction between the *circletail* (*Crc*) allele of *Scrib* and *looptail* (*Lp*) mice—in which a significant proportion of *Crc/+;Lp/+* double heterozygous embryos have a craniorachischisis defect similar to mice homozygous for each mutation alone—has previously been demonstrated (Murdoch *et al.* 2001). We

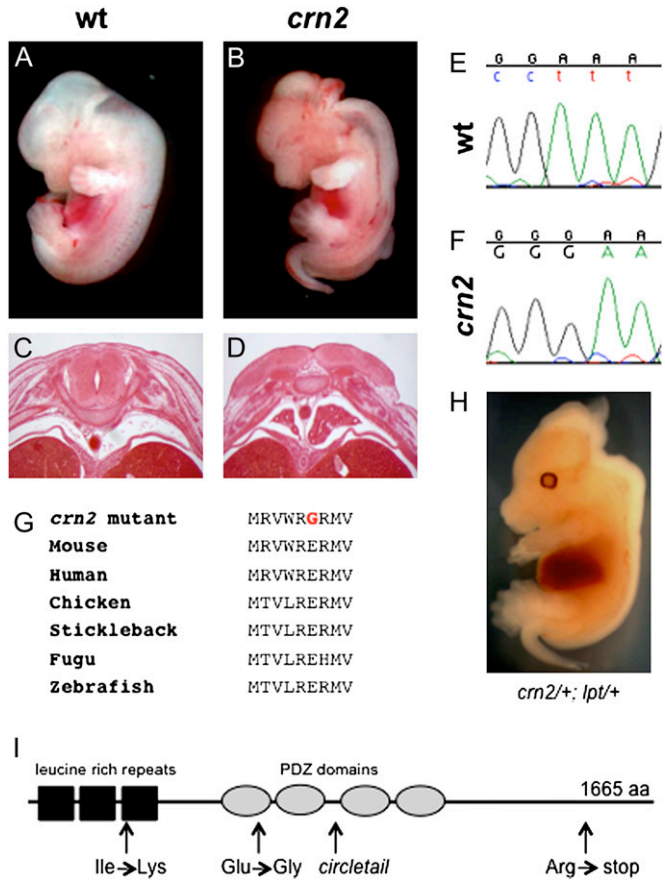

Figure 2 *Crn2* is a mutation in *scribble* gene. *Craniorachischisis2* mutants have an open neural tube (mid-hindbrain exencephaly and spina bifida aperta) and a curly tail (B and D). (C and D) Sections from the lumbar region. Sequence analysis of *crn2* transcript from wild-type (wt) embryos (E) and *crn2* mutants (F) revealed a mutation in a highly conserved residue (G) in the scribble protein. (H) *Crn2/+; lpt/+* double heterozygous embryos phenocopied the *crn2* phenotype. (I) A schematic summary of scribble mutations recovered to date (*see Results*).

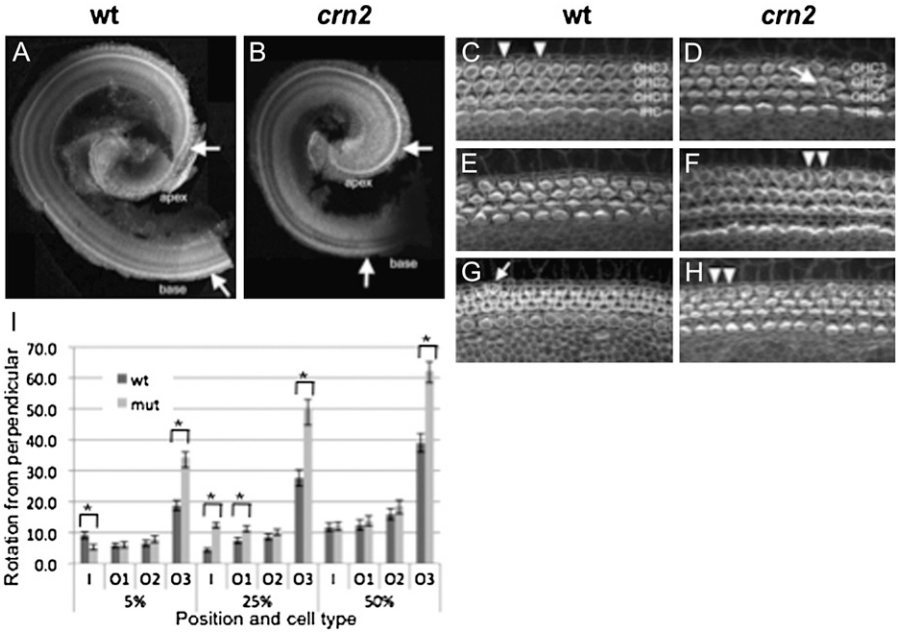

Figure 3 Cochlear hair-cell stereocilia patterning is abnormal in *cnr2* mutants. (A) Low-magnification view of wild-type (wt) E18 cochlear epithelium, stained with phalloidin to mark filamentous actin. The base and apex of the cochlear duct are indicated. (B) The cochlear duct from a *crn2* mutant was notably shorter, but overall morphology and patterning appeared normal. Arrows indicate the hair cells (HCs) within the sensory epithelium. (C) Wild-type cochlea at 5% of the total cochlear length from the base. A single row of inner HCs (IHC), and three rows of outer HCs (OHC1, -2, -3) were present. Stereocilia bundles were mostly oriented perpendicularly to the long axis of the cochlea. Some bundles in the third row of the outer HCs (OHC3) were slightly rotated (indicated by arrowheads). (D) *crn2* mutant cochlea, shown as in C, where OHC cellular patterning is comparable to the wild type. A single first-row OHC showed disrupted orientation (arrow). (E and F) Views of wild-type (E) and *crn2* (F) cochlea at 25%, similar to C and D. Greater disruptions in bundle orientations were apparent at this position, especially in the third row of OHC (arrowheads in F). (G and H) Wild-type (G) and *crn2* mutant (H) cochleae at 50%. The stereocilia bundles of both wild type and mutant HCs are less mature at this position, and more variability in stereocilia orientation was observed. Misoriented bundles were indicated in both wild type (G, arrow) and mutant (H, arrowheads). (I) Quantification of the hair-cell orientation defect in wild-type and *crn2* mutants is shown. I: IHC; O1, O2, O3: OHC1, -2, -3, respectively. $*P < 0.05$ is difference between the average angle of rotation of wild-type and *crn2* mutants.

performed the same cross with the *crn2* mice and also saw a strong genetic interaction with the *Lp* allele. We recovered four double heterozygote (*crn2/+; Lp/+*) embryos. Two of these had the full craniorachischisis defect (Figure 2H) and two had the looped-tail phenotype, a similar finding to the analysis of *Crc/+;Lp/+* mice (Murdoch *et al.* 2001).

While further breeding the *crn2* and *Lp* alleles on a highly mixed genetic background (A/J, FVB, 129, and B6), we noted a variable penetrance of the craniorachischisis phenotype. Some adult mice in this subpopulation are homozygous for the *crn2* mutation, and one affected embryo appears heterozygous. As several of these mice are derived from a parent in which a recombination event occurred proximal to *Scrib*, there is a formal possibility that there is a mutation that causes a phenotype that is phenotypically identical to *Scrib* and interacts similarly with *Lp*. However, the minimal recombinant interval derived from these mice and those originally studied reveals that it contains only one gene, *Efr3a*, and direct sequencing did not reveal a coding change. Furthermore, the amino acid mutated in *crn2* is conserved as a glutamic acid in all vertebrates examined, as well as in *Drosophila*. Multiple studies present evidence that penetrance of mouse neural-tube closure phenotypes can vary with genetic background in both mutations of planar cell polarity genes (Wang *et al.* 2006; Paudyal *et al.* 2010) and in other genes (Matteson *et al.* 2008). Given these findings, we believe that the variable phenotype of the *crn2* allele is a consequence of the mixed genetic background.

We also examined the cochlea of the *crn2* mutant as PCP is necessary for proper elongation of the developing cochlea and the stereotypical alignment of the stereocilia on the hair cells (Montcouquiol *et al.* 2003). We found that the cochlea had a normal morphology but was shorter in *crn2* mutants (Figure 3, A and B). Examination of the stereocilia on wild-type cochlear hair cells revealed them to be largely perpendicular to the long axis of the cochlea. In mutants, however, the stereocilia are less uniformly oriented (Figure 3, C–I). These results are consistent with the *crn2* mutation acting as a null or highly hypomorphic allele.

This is the fourth reported allele of *Scrib* (Figure 2I). The classic *circletail* mutation is a premature stop codon resulting in a protein of 971 amino acids and translation of only the first two of four PDZ domains (Murdoch *et al.* 2003). Two previous ENU screens have identified missense mutations in *Scrib*: one in a leucine-rich region 5′ of *Scrib* (Zarbalis *et al.* 2004) and one creating a premature stop eliminating 10% of the amino acid sequence (Wansleeben *et al.* 2010). The *crn2* mutation reported here is in the last amino acid of the first PDZ domain. The fact that all of these mutations cause such similar phenotypes suggests that multiple regions of the SCRIB protein are required for proper SCRIB function.

Hith2 is likely a novel allele of *caspase-3*

Hole in the head 2 (*hith2*) mutants were initially identified in the third arm of our screen focused on postnatal phenotypes. *Hith2* mutants have significant encephaloceles, some of which are visible through the skin of the postnatal pups (Figure 4, A–C), a phenotype very reminiscent of the *hith* mutation in *forkhead box c1* (*Foxc1*) (Zarbalis *et al.* 2007). We also noted an incompletely penetrant cleft palate phenotype in embryonic dissections. Most homozygous *hith2*

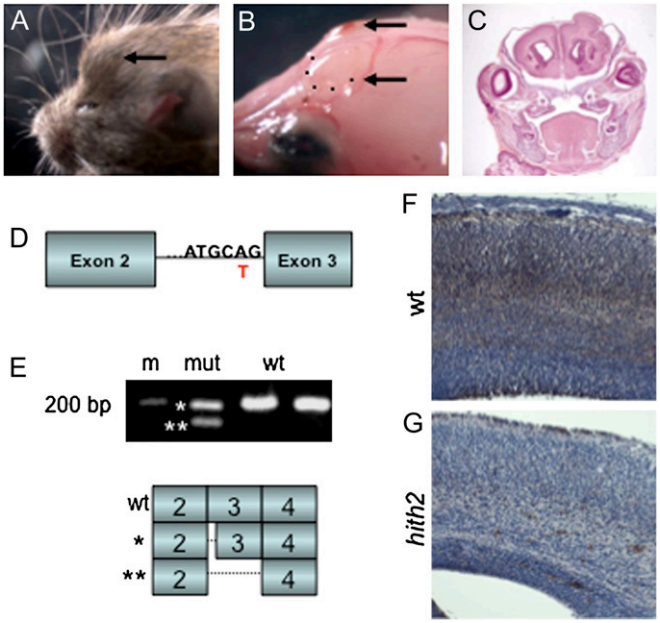

Figure 4 *Hole in the head 2* (*hith2*) is a mutation in *caspase-3*. *Hole in the head 2* (*hith2*) mutants had encephaloceles (often bilateral) first noted as tissue accumulated under the skin of the skull (arrow in A). (B) Further dissection revealed the encephaloceles (arrows; dotted line indicates border of open skull and neural tissue), which were easily visible with histological analysis (C). (D) Sequencing of the *caspase-3* locus identified a mutation in the intron between exons 2 and 3. (E) RT-PCR analysis of the *hith2* cDNA resulted in two PCR products. Direct sequencing of the larger (*) showed the transcript splices into the third exon downstream of the normal splice site. The smaller product (**) is a complete skipping of the third exon. Both *hith2* isoforms are predicted to generate missense proteins with a premature stop codon. Missing sequence is indicated by dotted lines. Immunohistochemistry for *caspase-3* confirms little or no protein in the *hith2* E17.5 cortex (G) as compared to wild type (wt) (F).

mutants do not survive past birth, and a substantial proportion of *hith2* heterozygous have an abnormal gait consistent with a vestibular defect.

We initially mapped the *hith2* mutation to chromosome 8 and identified *Casp3* as a candidate gene on the basis of the similarity to published phenotypes (Kuida *et al.* 1996; Takahashi *et al.* 2001; Leonard *et al.* 2002). Sequencing of the *Casp3* locus in the *hith2* embryos revealed a mutation in the intron between exons 2 and 3, two nucleotides upstream of the beginning of the third exon (Figure 4D). Subsequent cDNA analysis by RT-PCR showed the mutant transcript to have two isoforms. Sequencing the RT-PCR products revealed the larger of these products to be an imprecise splicing event four nucleotides into the third exon and the smaller species to be a complete skipping of the third exon (Figure 4E). Both alternate transcripts are predicted to result in missense proteins with premature stop codons. *Casp3* is an established effector of apoptotic cell death (Nijhawan *et al.* 2000), and full-length CASPASE-3 is normally cleaved into an active form during apoptotis. Consistent with the alternate transcripts that we identified, immunohistochemical analysis demonstrated that little or no CASPASE-3 is produced in *hith2* mutants (Figure 3G). Multiple alleles of *Casp3* have been created with similar phenotypes, four of which produce no protein (Kuida *et al.* 1996; Woo *et al.* 1998; Keramaris *et al.* 2000; Morishita *et al.* 2001), and a missense mutation at a catalytic residue (Parker *et al.* 2010).

Additional mutant characterization

Homozygous *rudolph* (*rud*) mutants had skeletal defects, craniofacial defects, and neural defects. Some of the mutants had an accumulation of fluid in a bleb at the end of the snout that sometimes filled with blood (Figure 5A). Histological analysis revealed severe differentiation defects throughout the central nervous system (Figure 5B; data not shown). We have identified a causal mutation on chromosome 1 in the cholesterol biosynthetic enzyme *hydroxysteroid (17-beta) dehydrogenase 7* (*Hsd17b7*) and further analysis of this mutation will be presented separately (R. W. Stottmann, H. Qiu, J. L. Moran, D. R. Beier, unpublished results).

We also recovered the *brain dimple* (*brdp*) mutation in this portion of the screen. *Brdp* mutants were grossly indistinguishable from wild-type littermates upon dissection at E18.5. Microdissection of the brain revealed defects in brain development, including smaller olfactory bulbs and a significant thinning of the caudo-lateral telencephalic tissue (Figure 5D). Mapping of this mutation suggests that it is a novel locus on chromosome 13.

Several of the mutations that we recovered had craniofacial phenotypes along with neural phenotypes. *Cleft palate and exencephaly* (*clpex*) mutants have multiple phenotypes at E18.5, including cleft lip, cleft palate, exencephaly, and closed brain cavities with a flattened head. The exencephaly and clefting phenotypes are incompletely penetrant and occur both independently and in the same embryo (Figure 5, F–H). One mutant exhibited spina bifida aperta. Mapping of the mutation identifies a likely novel locus on chromosome 7.

Cleft face (*clft3*) mutants were initially identified by the failure of the craniofacial tissue to fuse at the midline (Figure 5I). Further dissections revealed mutants with an accumulation of apparently vascularized tissue on top of the skull (Figure 5J). Mutant embryos were often smaller, and we saw many dead and dying embryos at mid-embryonic stages (data not shown). Histological analysis revealed that the brain of *clft3* mutants appears smaller than controls (Figure 5, K and L) and that the tissue on top of the cranium is encephaloceles where the neural tissue had grown through a patent surface ectoderm (data not shown). *Clft3* is an apparently novel allele of a gene on chromosome 15.

We recovered one line (*cleft palate 1*) (*clft1*) with cleft palate but no CNS defects. We have identified this to be a hypomorphic allele of the known clefting gene, *interferon regulatory factor 6* (*Irf6*) (Ingraham *et al.* 2006; Richardson *et al.* 2006; Stottmann *et al.* 2010).

The *progressive hydrocephaly* (*prh*) mutant was discovered in the third arm of the screen, although the phenotype is not dependent on heterozygosity at the *Lis1* locus. *Prh* mutants are indistinguishable from littermates at birth but

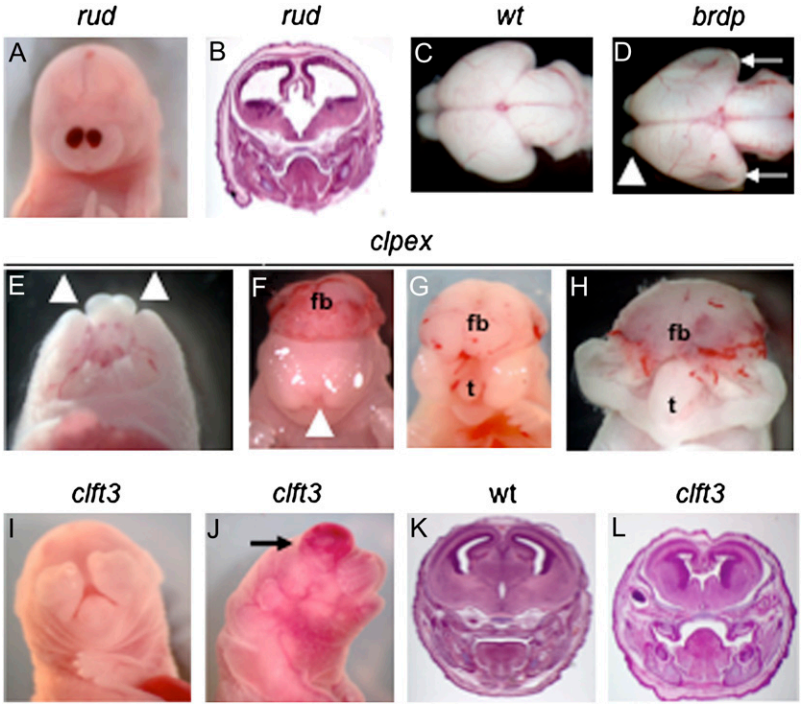

Figure 5 ENU mutants with craniofacial and neurodevelopmental defects. (A and B) *Rudolph* (*rud*) mutants were notable for the occasional accumulation of blood at the tip of the nose (A) and dramatic defects in brain organization (B). (C and D) *Brdp* brains are distinguished at E18.5 by their smaller olfactory bulbs (arrowhead) and by the significant thinning of the cortex visible at the caudal-most portion of the forebrain (arrows) as compared to wild type (wt). (E and F) *clpex* mutants show a range of craniofacial defects. (E) Ventral view of the craniofacial region of the *clpex* embryo with mandible removed indicates a bilateral cleft lip (arrowheads). (F–H) The most severe cases had both exencephaly and anterior craniofacial fusion defects. (G–L) *clft3* mutants were first noted for craniofacial fusion defects (I). Other defects include smaller-sized embryos, neuronal overmigration (arrow in J), cleft palate (L), and reduced forebrain size in mutants (L) as compared to wild type (K). fb: forebrain; t: tongue

are visibly hydrocephalic by P14 (Figure 6, B and F), are less vigorous, and do not survive to weaning ages. The hydrocephaly is not present at birth (Figure 6D), is first visible histologically at P7, and gradually increases in severity through the rest of life (data not shown). Ventricular dilation is visible in the lateral and third ventricles.

Discussion

We describe our recent efforts to expand the use of ENU mutagenesis in the mouse to uncover novel alleles in a particular tissue of interest, in this case, the forebrain. We used three strategies to increase the sensitivity of the screen for mutations with phenotypes relevant to neurodevelopment: (1) a morphological and histological analysis of the forebrain; (2) inclusion of a reporter allele, the RARE-lacZ transgene; and (3) the use of a sensitizing allele, *Lis1*.

We find that including various alleles into a traditional three-generation screen does not significantly increase the effort involved to generate and screen the mutant lines. Furthermore, the genetic heterogeneity introduced along with these modifying alleles can be accommodated and still allow rapid mapping of the mutations. However, as one might expect, this genetic heterogeneity can affect phenotype reproducibility; the RARE-lacZ reporter allele turned out to have variable expression in the backgrounds that we used, and no variants from that portion of the screen were proven heritable. The *Lis1*-sensitized portion of the screen also did not recover any novel interacting genes. However, in both of these cases, we were able to comprehensively analyze only a small number of lines with these modifications. In fact, the sensitized portion of our screen more realistically represents a pilot screen testing the approach of using a sensitizing locus with its own genetic background

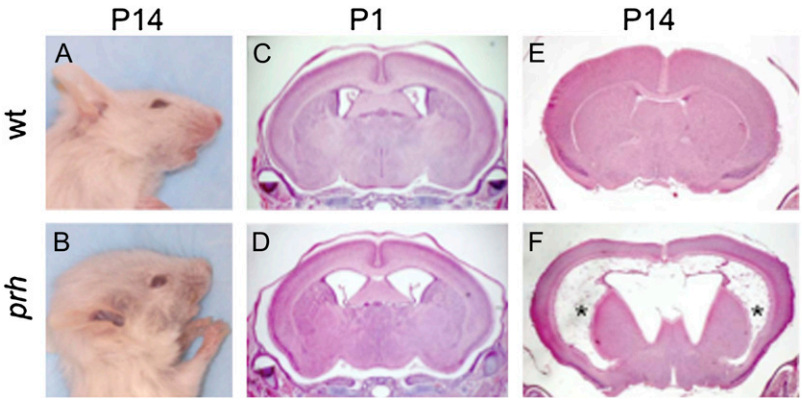

Figure 6 *Prh* mutants have postnatal phenotypes. *Prh* mutants were notable at P14 by their decreased size and domed head (B) as compared to wild type (A). Histological examination revealed severe hydrocephalus at P14 [in (F), ventriculomegaly is indicated by asterisks; wild type section shown in (E)]. Mutants did not have significant ventriculomegaly at P1 (C and D).

heterogeneity. Our experience shows that the addition of these components to the screen does not overly complicate the logistics and efficiency of the mutagenesis protocol and, with appropriate selection of alleles, can be an invaluable addition to the experimental design. In the experiment that we describe here, the most valuable approach was to dissect the brain and observe in whole mount. This was clearly fruitful, but is still a relatively blunt approach to observing neurodevelopment. We anticipate continuing to utilize reporter alleles targeting different aspects of neuronal development in future mutagenesis efforts. The continuing addition of transgenic mouse reagents to the neuroscience repertoire [*e.g.*, the GENSAT project (Gong *et al.* 2003)] provides a growing resource for reporter screens, further enhancing the utility of this approach.

Our attempt to refine the technique and query a specific organ was successful as seven of eight mutants that we recovered had some effect on forebrain development. We comprehensively screened only 38 families, giving a success rate in obtaining a neurodevelopmental mutant of 7/38 (18%). As five of these genes appear to be novel genes in forebrain developmental genetics, this continues to show that ENU mutagenesis is an efficient tool for gene discovery and compares favorably with other recent screening efforts. A previous approach in our own laboratory aimed at general morphological defects recovered 15 monogenic mutants in 54 lines [28% of lines comprehensively analyzed (Herron *et al.* 2002)]. A previous attempt to query neurodevelopment with a reporter of cortical tangential migration recovered 13 phenotypes from 305 lines (4% of all lines established) with 5 specific to the reporter allele used [1.6% (Zarbalis *et al.* 2004)]. Another reporter screen assaying axon guidance recovered 7 mutants from 57 lines (12%) with 6 affecting the reporter allele expression (Dwyer *et al.* 2011). A immunohistochemical approach to studying cranial nerve development yielded seven mutants from 40 pedigrees [18% (Mar *et al.* 2005)].

We report a novel allele of *Scrib*, which contributes to a greater understanding of this large protein. The scribble protein has leucine-rich repeats at the 5′ end and multiple PDZ protein interaction domains at the 3′ end. The premature stop generated by the initial *circletail* mutation is predicted to produce only the first two PDZ domains and indicated that the PDZ domains are critical for the function of the Scribble protein (Murdoch *et al.* 2003). Another ENU-induced mutation demonstrated that the leucine-rich regions are also critical (Zarbalis *et al.* 2004). A third allele, also from an ENU screen, retained ~90% of the coding sequence, but mRNA levels were reported to be down 65% (Wansleeben *et al.* 2010). Our *crn2* missense mutation is at the extreme 3′ end of the first PDZ domain and may prevent the full-length *Scrib* protein from folding correctly or interfere with other specific protein interactions. These alleles together support the notion that *Scrib* encodes a scaffolding protein in the PCP pathway with multiple important protein–protein interaction sites.

We have isolated several mutants of interest for neurodevelopment. All but one of the mutations that we report here were lethal at or before birth, suggesting that they each have pleiotropic effects, possibly leading to many other avenues of future investigation. Furthermore, our phenotype-driven analysis may have uncovered hypomorphic alleles for genes in which a true null allele would have led to early embryonic lethality. Thus, a reverse genetic, "knock-out allele" approach may not have implicated these genes in neurodevelopment. The imminent availability of a large set of conditionally targeted mutant ES lines should facilitate complementary studies of ENU alleles as they are generated (Collins *et al.* 2007).

Acknowledgments

We thank A. Tilt, H. Qiu, S. Hines, A. Bolton, and S. Nicholson for assistance in screening and mapping; M. Lun, Y. Yun, and M. Prysak for assistance with animal husbandry; and J. Min for assistance with caspase-3 immunohistochemistry. We thank U. Drager (University of Massachusetts Medical School) for the RARE-lacZ mouse line, Lisa Goodrich (Harvard Medical School) for the *looptail* mice, and A. Wynshaw-Boris (University of California at San Francisco) for the *Lis1* mouse. Funding for this project is from the National Institutes of Health (grants R01HD0306404 and R01MH081187 to D.R.B. and grant F32HD053198 to R.W.S.).

Literature Cited

Ackerman, K. G., B. J. Herron, S. O. Vargas, H. Huang, S. G. Tevosian *et al.*, 2005 Fog2 is required for normal diaphragm and lung development in mice and humans. PLoS Genet. 1: 58–65.

Assadi, A. H., G. Zhang, U. Beffert, R. S. McNeil, A. L. Renfro *et al.*, 2003 Interaction of reelin signaling and Lis1 in brain development. Nat. Genet. 35: 270–276.

Beckstead, W. A., B. C. Bjork, R. W. Stottmann, S. Sunyaev, and D. R. Beier, 2008 SNP2RFLP: a computational tool to facilitate genetic mapping using benchtop analysis of SNPs. Mamm. Genome 19: 687–690.

Bode, V. C., J. D. McDonald, J. L. Guenet, and D. Simon, 1988 *hph-1*: a mouse mutant with hereditary hyperphenylalaninemia induced by ethylnitrosourea mutagenesis. Genetics 118: 299–305.

Chiang, C., Y. Litingtung, E. Lee, K. E. Young, J. L. Corden *et al.*, 1996 Cyclopia and defective axial patterning in mice lacking Sonic hedgehog gene function. Nature 383: 407–413.

Collins, F. S., J. Rossant, and W. Wurst, 2007 A mouse for all reasons. Cell 128: 9–13.

Dwyer, N. D., D. K. Manning, J. L. Moran, R. Mudbhary, M. S. Fleming *et al.*, 2011 A forward genetic screen with a thalamocortical axon reporter mouse yields novel neurodevelopment mutants and a distinct emx2 mutant phenotype. Neural Dev 6: 3.

Gambello, M. J., D. L. Darling, J. Yingling, T. Tanaka, J. G. Gleeson *et al.*, 2003 Multiple dose-dependent effects of Lis1 on cerebral cortical development. J. Neurosci. 23: 1719–1729.

Gong, S., C. Zheng, M. L. Doughty, K. Losos, N. Didkovsky *et al.*, 2003 A gene expression atlas of the central nervous system based on bacterial artificial chromosomes. Nature 425: 917–925.

Hebert, J. M., and S. K. McConnell, 2000 Targeting of cre to the Foxg1 (BF-1) locus mediates loxP recombination in the telencephalon and other developing head structures. Dev. Biol. 222: 296–306.

Herron, B. J., W. Lu, C. Rao, S. Liu, H. Peters *et al.*, 2002 Efficient generation and mapping of recessive developmental mutations using ENU mutagenesis. Nat. Genet. 30: 185–189.

Hirotsune, S., M. W. Fleck, M. J. Gambello, G. J. Bix, A. Chen *et al.*, 1998 Graded reduction of Pafah1b1 (Lis1) activity results in neuronal migration defects and early embryonic lethality. Nat. Genet. 19: 333–339.

Ingraham, C. R., A. Kinoshita, S. Kondo, B. Yang, S. Sajan *et al.*, 2006 Abnormal skin, limb and craniofacial morphogenesis in mice deficient for interferon regulatory factor 6 (Irf6). Nat. Genet. 38: 1335–1340.

Kasarskis, A., K. Manova, and K. V. Anderson, 1998 A phenotype-based screen for embryonic lethal mutations in the mouse. Proc. Natl. Acad. Sci. USA 95: 7485–7490.

Keramaris, E., L. Stefanis, J. MacLaurin, N. Harada, K. Takaku *et al.*, 2000 Involvement of caspase 3 in apoptotic death of cortical neurons evoked by DNA damage. Mol. Cell. Neurosci. 15: 368–379.

Kuida, K., T. S. Zheng, S. Na, C. Kuan, D. Yang *et al.*, 1996 Decreased apoptosis in the brain and premature lethality in CPP32-deficient mice. Nature 384: 368–372.

Leonard, J. R., B. J. Klocke, C. D'Sa, R. A. Flavell, and K. A. Roth, 2002 Strain-dependent neurodevelopmental abnormalities in caspase-3-deficient mice. J. Neuropathol. Exp. Neurol. 61: 673–677.

Luo, T., E. Wagner, F. Grun, and U. C. Drager, 2004 Retinoic acid signaling in the brain marks formation of optic projections, maturation of the dorsal telencephalon, and function of limbic sites. J. Comp. Neurol. 470: 297–316.

Mar, L., E. Rivkin, D. Y. Kim, J. Y. Yu, and S. P. Cordes, 2005 A genetic screen for mutations that affect cranial nerve development in the mouse. J. Neurosci. 25: 11787–11795.

Matteson, P. G., J. Desai, R. Korstanje, G. Lazar, T. E. Borsuk *et al.*, 2008 The orphan G protein-coupled receptor, Gpr161, encodes the vacuolated lens locus and controls neurulation and lens development. Proc. Natl. Acad. Sci. USA 105: 2088–2093.

McDonald, J. D.,, and V. C. Bode, 1988 Hyperphenylalaninemia in the hph-1 mouse mutant. Pediatr. Res. 23: 63–67.

Meyers, E. N., M. Lewandoski, and G. R. Martin, 1998 An Fgf8 mutant allelic series generated by Cre- and Flp-mediated recombination. Nat. Genet. 18: 136–141.

Mishina, Y., A. Suzuki, N. Ueno, and R. R. Behringer, 1995 Bmpr encodes a type I bone morphogenetic protein receptor that is essential for gastrulation during mouse embryogenesis. Genes Dev. 9: 3027–3037.

Montcouquiol, M., R. A. Rachel, P. J. Lanford, N. G. Copeland, N. A. Jenkins *et al.*, 2003 Identification of Vangl2 and Scrb1 as planar polarity genes in mammals. Nature 423: 173–177.

Morishita, H., T. Makishima, C. Kaneko, Y. S. Lee, N. Segil *et al.*, 2001 Deafness due to degeneration of cochlear neurons in caspase-3-deficient mice. Biochem. Biophys. Res. Commun. 284: 142–149.

Murdoch, J. N., R. A. Rachel, S. Shah, F. Beermann, P. Stanier *et al.*, 2001 Circletail, a new mouse mutant with severe neural tube defects: chromosomal localization and interaction with the loop-tail mutation. Genomics 78: 55–63.

Murdoch, J. N., D. J. Henderson, K. Doudney, C. Gaston-Massuet, H. M. Phillips *et al.*, 2003 Disruption of scribble (Scrb1) causes severe neural tube defects in the circletail mouse. Hum. Mol. Genet. 12: 87–98.

Nagy, A., 2003 Manipulating the Mouse Embryo: A Laboratory Manual. Cold Spring Harbor Laboratory Press, Cold Spring Harbor, NY.

Nijhawan, D., N. Honarpour, and X. Wang, 2000 Apoptosis in neural development and disease. Annu. Rev. Neurosci. 23: 73–87.

Parker, A., R. E. Hardisty-Hughes, L. Wisby, S. Joyce, and S. D. Brown, 2010 Melody, an ENU mutation in Caspase 3, alters the catalytic cysteine residue and causes sensorineural hearing loss in mice. Mamm. Genome 21: 565–576.

Paudyal, A., C. Damrau, V. L. Patterson, A. Ermakov, C. Formstone *et al.*, 2010 The novel mouse mutant, chuzhoi, has disruption of Ptk7 protein and exhibits defects in neural tube, heart and lung development and abnormal planar cell polarity in the ear. BMC Dev. Biol. 10: 87.

Rachel, R. A., J. N. Murdoch, F. Beermann, A. J. Copp, and C. A. Mason, 2000 Retinal axon misrouting at the optic chiasm in mice with neural tube closure defects. Genesis 27: 32–47.

Reiner, O., R. Carrozzo, Y. Shen, M. Wehnert, F. Faustinella *et al.*, 1993 Isolation of a Miller-Dieker lissencephaly gene containing G protein beta-subunit-like repeats. Nature 364: 717–721.

Richardson, R. J., J. Dixon, S. Malhotra, M. J. Hardman, L. Knowles *et al.*, 2006 Irf6 is a key determinant of the keratinocyte proliferation-differentiation switch. Nat. Genet. 38: 1329–1334.

Rossant, J., R. Zirngibl, D. Cado, M. Shago, and V. Giguere, 1991 Expression of a retinoic acid response element-hsplacZ transgene defines specific domains of transcriptional activity during mouse embryogenesis. Genes Dev. 5: 1333–1344.

Stottmann, R. W.,, and D. R. Beier, 2010 Using ENU mutagenesis for phenotype-driven analysis of the mouse. Methods Enzymol. 477: 329–348.

Stottmann, R. W., B. C. Bjork, J. B. Doyle, and D. R. Beier, 2010 Identification of a Van der Woude syndrome mutation in the cleft palate 1 mutant mouse. Genesis 48: 303–308.

Takahashi, K., K. Kamiya, K. Urase, M. Suga, T. Takizawa *et al.*, 2001 Caspase-3-deficiency induces hyperplasia of supporting cells and degeneration of sensory cells resulting in the hearing loss. Brain Res. 894: 359–367.

Wang, J., N. S. Hamblet, S. Mark, M. E. Dickinson, B. C. Brinkman *et al.*, 2006 Dishevelled genes mediate a conserved mammalian PCP pathway to regulate convergent extension during neurulation. Development 133: 1767–1778.

Wansleeben, C., H. Feitsma, M. Montcouquiol, C. Kroon, E. Cuppen *et al.*, 2010 Planar cell polarity defects and defective Vangl2 trafficking in mutants for the COPII gene Sec24b. Development 137: 1067–1073.

Weber, J. S., A. Salinger, and M. J. Justice, 2000 Optimal N-ethyl-N-nitrosourea (ENU) doses for inbred mouse strains. Genesis 26: 230–233.

Woo, M., R. Hakem, M. S. Soengas, G. S Duncan, A. Shahinian *et al.*, 1998 Essential contribution of caspase 3/CPP32 to apoptosis and its associated nuclear changes. Genes Dev. 12: 806–819.

Zarbalis, K., S. R. May, Y. Shen, M. Ekker, J. L. Rubenstein *et al.*, 2004 A focused and efficient genetic screening strategy in the mouse: identification of mutations that disrupt cortical development. PLoS Biol. 2: E219.

Zarbalis, K., J. A. Siegenthaler, Y. Choe, S. R. May, A. S. Peterson *et al.*, 2007 Cortical dysplasia and skull defects in mice with a Foxc1 allele reveal the role of meningeal differentiation in regulating cortical development. Proc. Natl. Acad. Sci. USA 104: 14002–14007.

Communicating editor: T. R. Magnuson